Volume 1 | Number 1 | Jan 2013 | Pages 1–100

Journal of
Materials Chemistry C

Materials for optical and electronic devices
www.rsc.org/materialsC

ROYAL SOCIETY
OF CHEMISTRY

ROYAL SOCIETY
OF CHEMISTRY

www.rsc.org/materialsC

ARTICLE TYPE

White Light Emitting Single Polymer from Aggregation Enhanced Emission: A Strategy through Supramolecular Assembly

Ezhakudiyan Ravindran,ab Soundaram Jeevarathinam Ananthakrishnan,ab Elumalai Varathan,abc Venkatesan Subramanian,abc Narayanasastri Somanathan*abc †

5

Aggregation Induced Emission Enhancement (AIEE) is widely regarded as an efficient tool to offset the problem of Aggregation Caused Quenching (ACQ) in luminogens. ACQ phenomenon in small organic
10 molecules and polymers are detrimental to the performance of OLEDs. An efficient pure white electroluminescence (EL) was obtained by copolymerization of 9,9-dihexylfluorene as a blue host with (E)-2,7-dibromo-9H-fluoren-9-yl-2-cyano-3-(dimethylamino)phenyl)acrylate (FCP) as a yellow emitting covalent dopant with AIEE property on the main chain of the copolymers have been designed and synthesized. White light emission was achieved in copolymer FCP 2.5 that contained 2.5% of the AIEE
15 luminogen. Interestingly the copolymers exhibited enhanced emission upon aggregation even in low composition of FCP. The enhanced emission in the copoloymers is attributed to the supramolecular assembly of polymeric chains. A density functional (DFT) and time-dependent density functional theory (TD-DFT) investigation on the monomer and copolymers of FCP revealed that the presence of an intramolecular charge transfer (ICT) transition between dimethylamine to cyanoacrylic acid unit.
20 OLEDs were fabricated using device with the structure of ITO/PEDOT:PSS/EML/Al. White light emitting diodes were fabricated from FCP 2.5 as a Emissive layer (EML) elicited a white electroluminescence with *Commission internationale de l'Eclairage* (CIE) of (0.33, 0.34) and shows the maximum brightness of nearly 9332 cd m^{-2}, power efficiency of 4.13 lm W^{-1}, luminous efficiency of 6.34 cd A^{-1}. Interestingly, the supramolecular ordering in FCP 2.5 considerably reduces the charge trapping
25 which results in reproducible white light emission.

Introduction

Organic light emitting diodes (OLEDs) present a hitherto different possibility of lighting architecture signifying a departure from conventional point source lighting. Owing to their high
30 energy efficiency and robustness they are envied as a potential candidate of general lighting in near future. OLEDs differ from the conventional lighting sources by the fact that the injected charge carriers are converted into excitons that in turn lead to light emission.[1-7] White light emission through simple device
35 architecture of OLEDs have been received seminal importance from researchers.[8] A Myriad of strategies were devised by researchers for efficient white light emission from polymer based devices. The proposed strategies include multilayer architecture with blend of different emitting polymers, multilayer
40 phosphorescent emitters, single layer polymer blend and polymer host with fluorescent or phosphorescent small molecule dopant system.[9-13] Apart from the above conventional approaches, a few innovative schemes like supramolecular hydrogen bonding[14] and excited state intra molecular proton transfer were also reported.[15]
45 However the above systems suffered from intrinsic phase separation problem during long-term device function, variable mobilities of charge carriers with resultant alteration of

recombination zone due to the complicated fabrication resulting in voltage-dependent electroluminescence (EL).[16]
50 A single polymer white EL is highly desirable since it has advantages such as phase stability and cost effective upscaling of OLED fabrication.[17-19] Tailoring stable and efficient organic light emitting materials with various optoelectronic properties is paramount for achieving a breakthrough. In a white light emitting
55 polymer the chromophores can either be attached to the main chain or side chain.[20,21] Copolymer based WOLEDs can also be classified as those based on primary colour mixing or complimentary colour mixing.[22] After first white light emitting polymer was reported, some innovative strategies were developed
60 for such materials aimed at enhanced device performance including incorporation of triplet emitting metal complexes in main chain as well as side chain of polymers.[23-25] A majority of the reported white light emitting systems exhibited a significant difference of electroluminescence (EL) from photoluminescence
65 (PL) with reduction in efficiency of OLEDs. The above undesired effect was largely attributed to charge trapping. Charge trapping also resulted in superfluous energy cascade that could only
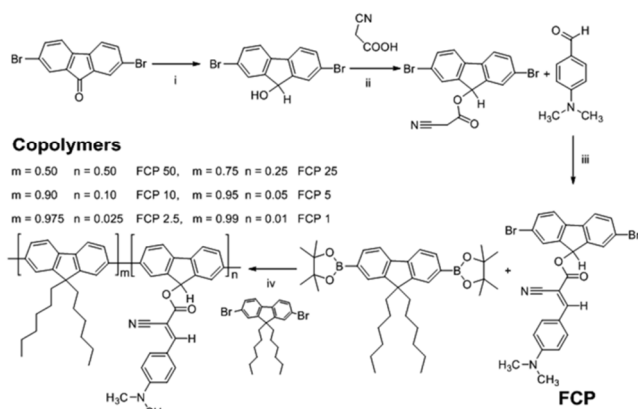
Scheme 1. Synthetic route to AIE monomer FCP and Suzuki polymerization with varying composition of FCP unit. (i) NaBH4, RT Stirring for 3 hrs. (ii) DCC / DMAP, RT stirring for 24 hrs. (iii) Pyridine, 5 83 ºC, Reflux for 24h. (iv) Pd(pph₃)₄ / NaHCO₃ Reflux for 72 hrs.

partially offset by low composition of dopant units in polymer chain. Nevertheless, researchers have highlighted the possibility of offsetting the charge trapping by use of bipolar emitters.[26]

10 Aggregation Induced Emission (AIE) phenomenon was recently introduced as an effective tool to offset the problem of ACQ.[27] Aggregation Caused Quenching (ACQ) in organic luminogens caused reduced emission in solid state consequently limiting practical application in OLEDs.[28,29] Ever since the initial discovery, AIE has continued to emerge as an important topic of

15 research.[30] Incorporation of AIE luminophores to the conjugated polymer backbone resulted in twisted structure thereby transferring the AIE property to the polymer.[31] AIE luminogens have found a myriad of applications like chemo/bio sensors, explosive detection, cell imaging and photo memory.[32,33]

20 Polymers with AIE moiety were also demonstrated as down conversion layer for white light emitting diode and as emissive layer for monochromatic Polymeric LEDs.[34] Supramolecular π-gel forming pyridinium salt was also reported with AIE property and white light emission albeit with temperature dependence.[35]

25 As a general criterion, AIE systems were tailored by the principle of restricted intramolecular rotation (RIR) to reduce π-π stacking interaction in solid state.[27] Some of the general structural components of AIE luminogens included tetraphenyl ethylene, polyphenyl ethylenes/cyano stilbene, polyphenyl

30 thiophenes/siloles, triphenyl pyridines and other geometrically hindered systems.[36] However, white light emission from a polymer containing AIE luminogenic moieties are still seldom reported. In this report we demonstrate a simple and novel strategy for white light emission from single copolymer of yellow

35 emitting AIE luminogen, (E)-2,7-dibromo-9H-fluoren-9-yl-2-cyano-3-diethylamino) phenyl) acrylate (FCP) and blue host 9,9-dihexyl-2,7-dibromofluorene (DHF) (Scheme 1). The electroluminescence of OLEDs was studied at varying compositions of the copolymers. Results from X-ray diffraction,

40 Atomic force microscopy and Scanning electron microscopy showed that the AIEE property of copolymers is due to the formation of supramolecular J-aggregates under device conditions. An efficient white light emission is demonstrated in a single polymer, FCP 2.5 as emissive layer in OLED with device

45 configuration of ITO/PEDOT:PSS/EML/Al. To the best of our

knowledge, the copolymer, FCP 2.5 with AIEE property represents a unique class of AIEE polymeric system with high purity white light emission and supramolecular assembly.

Results and Discussion

50 **Spectral properties of monomer and polymer**

Spectral properties of monomer and copolymers were studied in solution and thin film state (Figure 1). The absorption spectrum of FCP monomer in chloroform showed a strong absorption peak at 433 nm due to charge transfer transition and a shoulder at 286

55 nm due to π-π* transition. The copolymers elicited a change in wavelength of absorption with the various composition of FCP unit in the main chain of copolymers.
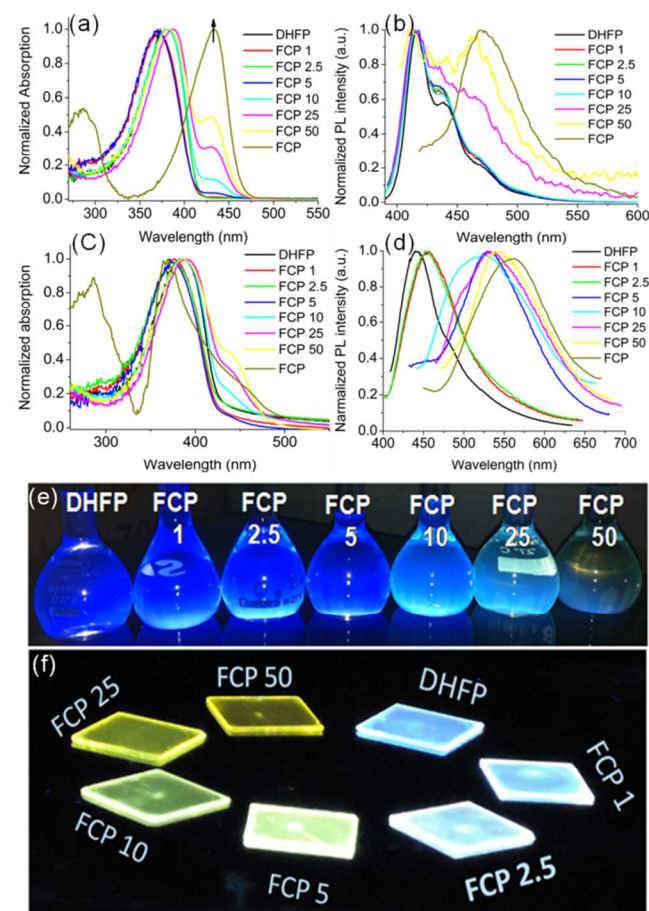

Figure 1. Absorption and PL spectra of FCP monomer and copolymers 60 in solutions (a) and (b), in thin films (c) and (d); (e) THF solutions and (f) Spun thin film of copolymers under irradiation at ~360 nm.

In the solution state, the absorption peaks were observed at 374 and 380 nm for FCP 1 and FCP 2.5 which have low composition of FCP units and can be assigned to be π-π* transition along the

65 conjugated backbone. The π-π* transitions of FCP 5, FCP 10, FCP 25, and FCP 50 (with higher FCP content in main chain) were observed at 373, 380, 386 and 383 nm respectively. The above polymers elicited a low energy shoulder observed at around 432 nm that is characteristic of FCP units was

70

Table 1. Spectral properties of monomer and polymers.

Polymer	$^a\lambda_{max}$ (Abs) (nm)		$^c\lambda_{max}$ (Emi) (nm)		$^d\Phi_{PL}{}^{SOL}$	$^e\Phi_{PL}{}^{TF}$
	Solution $^b(\varepsilon)$	Thin film	Solution (Exc)	Thin film (Exc)		
DHFP	380 (2.69x103)	384	416 (380)	441 (384)	71.7	64.8
FCP 1	373 (1.14 x103)	376	416 (373)	457 (376)	69.8	67.3
FCP 2.5	380 (1.13 x103)	375	415 (380)	455 (375)	65.7	71.5
FCP 5	370 (1.14x103), 432 (0.50 x102)	375, 437	415 (370)	531 (375)	50.4	65.7
FCP 10	380 (1.87 x103), 433 (2.18 x102)	385 , 438	415 (380)	526 (385)	20.9	54.7
FCP 25	386 (2.45 x103) 431 (7.60 x102)	389, 442	416, 467 (386)	533 (3890	0.55	66.1
FCP 50	383 (1.90 x103) ,431(9.20 x102)	386 , 443	413, 468 (383)	539 (386)	0.55	62.4
FCP	286 (11.6 x102), 433 (2.17x103)	286, 370, 455	470 (433)	562 (370)	0.01	73.4

$^a\lambda_{max}$ (Abs), Absorption maxima for Solution and Thin film in nm; $^b(\varepsilon)$, extinction coefficient in dL g^{-1} cm^{-1}. $^c\lambda_{max}$ (Emi), Emission maxima for Solution and Thin film in nm. $^d\Phi_{PL}{}^{SOL}$, The relative PL quantum yields were measured using quinine sulphate as a reference in THF solution, $^e\Phi_{PL}{}^{TF}$, The absolute PL quantum yields were measured using an integrating sphere.

prominently observed due to its relatively higher composition in backbone. In dilute solution of FCP monomer intermolecular rotations are allowed due to relatively low intramolecular rotation[37] and as a result of enhanced charge transfer (CT) between the electron rich N, N-dimethyl amine and electron deficient cyano segments.[38] The thin film absorption profile of FCP monomer and all copolymers showed π-π* transitions very close to their corresponding solution values (Figure 1(c)). The CT band of copolymers were observed at ~ 443 nm, slightly red shifted by up to 12 nm relative to solution absorption. In the case of monomer ~~as~~ there was no observable change in π-π* transitions. Nevertheless, FCP monomer elicited an anomalous change of absorption in the long wavelength region. The thin film spectrum of FCP monomer exhibited a new absorption peak at 370 nm with predominantly high intensity and the CT band was red shifted to 455 nm with significantly low intensity. The above observations can be interpreted as appearance of intramolecular twisted geometric form of FCP that elicited absorption peak at 370 nm alongside the (CT) band that appeared at 455 nm.[39] Similar observations were reported by researchers for systems with hybrid localized charge transfer (HLCT) .[40]

The normalized photoluminescence (PL) spectra of the copolymers in solution and thin film state revealed some significant information in the mode of energy transfer within the copolymer. In FCP, it includes two emitters: fluorene and cyano stilbene derivative. The blue emission may originate from fluorene in solution, and the yellow emission may be determined by AIE-active cyano stilbene derivative in aggregate. In solution state, the copolymer FCP 50, FCP 25 (higher composition of FCP unit) exhibited two characteristic emission peaks that correspond to the emission of poly (9,9-dihexylfluorene)-2,7-diyl (DHFP) centred at 416 and 413 nm.[41] In addition to the above emission peaks, FCP 50, FCP 25 copolymers elicited emission peaks at 467 and 468 nm respectively that closely correspond to that of FCP units. The presence of emission peak that correspond to FCP units in case of FCP 50, FCP 25 clearly indicate that there is a partial energy transfer from DHFP units to FCP units. Interestingly the FCP monomer exhibited a very low PL quantum yield of 0.01% in solution and a high quantum yield of 73.4% in thin film that is very characteristic of an AIE system (Table 1).[42] The observed low quantum yield in solutions of FCP 50, FCP 25 (with values of 0.54%, 0.55% respectively) despite the high quantum yield of DHFP (71.70% in solution) can be attributed only to the energy transfer to FCP monomer that in turn elicited very low quantum yield in solution state. In this context, the above observation can be compared with the earlier reports that showed low quantum yield for systems with AIE property in solution state.[42] Copolymers with low composition of FCP monomer (FCP 10-FCP 1) showed complete blue emission in solution state, the emission peaks appear at around 416 nm that is similar to emission of DHFP.

In thin film, the emission spectrum of copolymer was totally different from that of solution state. The copolymer FCP 1 and FCP 2.5 showed bathochromic shift (~ 16 nm) from DHFP, with emission at 456 nm. In addition to the above, FCP 1 and FCP 2.5 elicited enhanced quantum yield of 67.3% and 71.5% respectively (Table 1). It is also interesting to note that the emission of FCP 1 and FCP 2.5 were extended up to above 600 nm. From the above results it is clear that the change in emission properties of FCP1 and FCP 2.5 is due to partial energy transfer to FCP moieties. As a result of a high quantum yield of FCP units in thin films, pure white light emission was observed for FCP 2.5 while blue tinged and yellow tinged white light emission was observed for FCP 1 and FCP 5 respectively (Table 1 and Figure 1 (f)). The copolymers from FCP 10, FCP 25 and FCP 50 exhibited yellow emission at 526, 533, and 539 nm respectively with considerable bathochromic shift and high quantum yield compared to their respective solutions. FCP monomer elicited a high quantum yield of 73.4% in thin film and hence the enhanced quantum yield of all copolymers in thin film state is the direct consequence of enhanced emission of FCP units. Thus the enhanced emission of FCP monomer in thin film state and low

emission in solution state is characteristic of a typical AIE system.

Solvatochromic Study

Solvatochromism is a characteristic behaviour of dipolar molecules. In general, different polarity of solvent provides a useful frame work for studying solvent dependent spectral shift. Using Lippert- Mataga study the influence of different polarity of solvent environment on photo physical property of organic luminogen can be understood.[43] Lippert-Mataga study reveals that the interactions between the solvent and dipole moment of solute by using stoke's shift as a function of orientational polarizability.
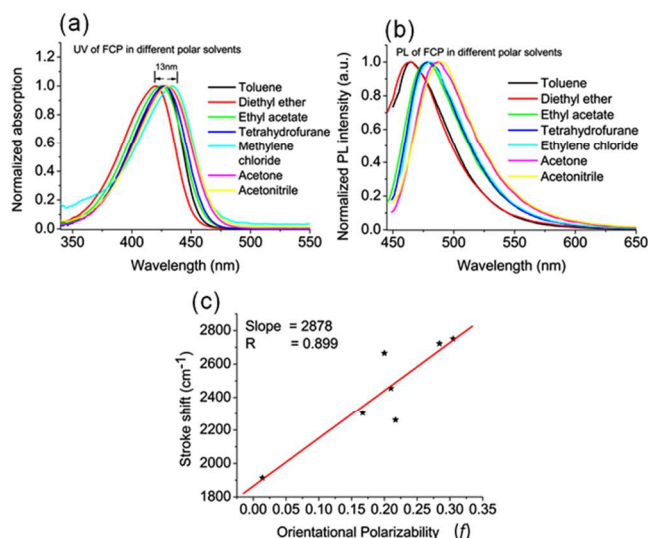

Figure 2. (a) and (b) absorption and PL spectra of FCP, done in different solvents with increasing polarity (The orientational polarizability of different solvent *(f)* given in Table S2†); (c) Linear correlation of orientation polarization *(f)* of solvent media with the Stokes shift (v a $- v$ f) for FCP.

The spectral properties of FCP monomer was studied as a function of orientational polarizability (*f*) by plotting stoke's shift against (*f*). Since orientational polarizability roughly corresponds to the amount of solvating power and interaction of solvent with solute, it can be used to study the photo-physical properties of luminogens. As an interesting observation, the absorption maxima of FCP in different solvents elicited a bathochromic shift of about 13 nm when the solvent was changed from toluene to acetonitrile (Figure 2). The emission spectra of FCP also showed a uniform bathochromic shift with increase in solvent polarity. A plot of Stoke's shift versus orientational polarizability (*f*), exhibited a high positive slope of 2878 and a linear correlation coefficient (R) of 0.899. The above observation indicated that the transitions responsible for yellow emission of FCP consists of significant charge transfer (CT) characteristic and involves high transition dipole moment. Thus the emission property of FCP is very sensitive to the microenvironment.

Dynamic light scattering and Fluorescence decay of Excited State

The aggregation properties of AIE luminophore incorporated copolymers were studied by Dynamic light scattering (DLS) experiment and Fluorescence lifetime analysis (FLT).[44, 45] The size distribution of the aggregates in solution were studied. The copolymers exhibited significant change in aggregation due to varying composition of FCP monomer. Dynamic light scattering studies revealed a bimodal distribution of particle sizes for all copolymer except white light emitting copolymer FCP 2.5 (Table 2). The copolymer, FCP 2.5 elicited a hydrodynamic radius of 566 nm with unimodal distribution. The above observation can be correlated indirectly with the spherical structures observed in AFM and SEM of copolymers (Figure 5). It can be clearly understood that the composition of FCP monomer is responsible for intermolecular interactions.[46] Previous studies have revealed that the aggregation characteristics in solution state can be transferred on to films cast from the solution. [47, 53]

Table 2. Fluorescence Life Time (FLT) and Dynamic Light Scattering (DLS) data of copolymers.

| Polymer | Fluorescence life time' | | | | DLS |
| | Solution | Thin film | | | |
	[a]τ_1/τ_2 (a$_1$/a$_2$)	[b]T_1/T_2 (A$_1$/A$_2$)	[c]χ^2		[d]R$_H$ (I)
DHFP	6.3/0.57 (1.2/98.8)	4.2/0.29 (12.08/87.92)	0.94/0.86		371 (100)
FCP 1	5.4/0.62 (1.37/98.63)	4.3/0.40 (14.87/85.13)	1.12/1.06		482.4/46.14 (93.6/6.4)
FCP 2.5	3.2/0.63 (3.72/96.28)	4.2/0.67 (17.17/82.83)	1.07/0.86		566.3 (100)
FCP 5	5.0/0.66 (19.09/80.96)	9.2/3.7 (24.49/75.51)	1.08/1.09		272/13.54 (87.9/12.1)
FCP 10	4.8/0.58 (22.08/77.92)	9.5/2.7 (70.74/29.26)	1.05/1.09		203.7/9.56 (91.3/8.7)
FCP 25	5.1/1.3 (48.33/51.67)	11.6/3.1 (71.92/28.08)	1.10/1.16		342/14.81 (77.45/22.55)
FCP 50	7.4/3.6 (57.89/42.11)	9.0/2.8 (73.68/26.33)	1.03/1.01		234/16.71 (58.57/41.43)

[a]τ_1/τ_2, Life time of different decay channels from FLT experiment in ns; a$_1$/a$_2$, % Contribution of different decay channels in solution. [b]T_1/T_2 Life time of different decay channels from FLT experiment in ns; A$_1$/A$_2$, % contribution of different decay channels in thin film. [c]χ^2, Correlation of exponential fit. [d]R$_H$, Hydrodynamic Radii in nm; I, % composition of different species with corresponding R$_H$ values.

Fluorescence decay of copolymers was measured in solution and solid state to identify the effect of aggregation on decay dynamics of excited state. The time correlated fluorescence decay analysis revealed that the average lifetime of excited states gradually
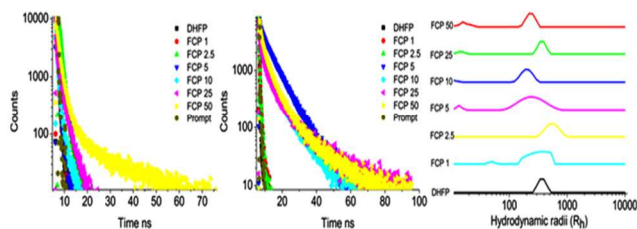

Figure 3. (a) and (b) Fluorescence lifetime decay of Copolymers in solution and thin film; (c) Dynamic light scattering traces of copolymers.

increased (in solution and thin film state) with the composition of FCP unit in copolymers. Table 2 summarizes fluorescence decay analysis in THF solution and solid films at room temperature. All the polymers elicited bi-exponential fluorescence decay in nanosecond range. Such bi-exponential decays are characteristic of the polymers with π- π* transition and intramolecular charge transfer (ICT) state. The observed composition of short lived and delayed decay channels of the copolymers can be correlated to the amount of aggregated and non-aggregated states.[47] The above correlation is possible since there is an efficient energy transfer to FCP units in the aggregates than in solvated molecules.

In solution state, the polymers with low percentage of FCP units showed a unique ultrafast decay channel which was very similar to that observed in DHFP used as a control for this study. The ultrafast decay channel with life time < 1ns can be correlated with the non-emissive states and also these ultrafast channels predominate in solutions of DHFP and copolymers, FCP 1 to FCP 10.[48] The ultrafast decay channel was not observed for copolymers FCP 25 and FCP 50. The copolymer FCP 25 and FF 50 elicited two decay channels in solution with longer average life time (Table 2 and Figure 3). In thin films, DHFP, FCP 1 and FCP 2.5 exhibited bi-exponential fluorescence decay with ultrafast decay channel, which is closely comparable with the solution. In contrast, the copolymers FCP 5 to FCP 50 elicited biexponential decay with increase in average lifetime of the above decay channels with composition of FCP unit (Table 2, Figure (a), (b)). The average lifetime of copolymer FCP 5 to FCP 50 increase as compared to the solution life time and thus signify that above observation can be attributed to the aggregation and enhanced emission in solid state.

Aggregation Induced Emission Enhancement properties

Incorporation of cyanovinyl functionality into the structural designing of multifunctional materials is a potential strategy to achieve efficient solid state lighting.[49] AIEE properties of FCP monomer and its copolymers were studied by adding a non-solvent into a solvent medium. In this experiment, water and THF were chosen as the solvent pairs to create different admixtures of varying compositions. The AIEE behaviour was examined by monitoring the changes in PL with the change in proportion of water in THF. The copolymers with major composition of FCP monomer, FCP 50 and FCP 25 elicited weak or no emission when molecularly dissolved in good solvent (THF). Interestingly, the monomer FCP and its copolymers FCP 50, FCP 25 and FCP 10 exhibited high quantum yield upon aggregation in presence of higher percentage of water fraction (f_w) in THF/water mixtures. In this experiment, the resultant mixture of THF/water with monomer and polymers were visually transparent and macroscopically identical, suggesting that the FCP monomer aggregates have nanometre size [50] (Figure 4(e)).
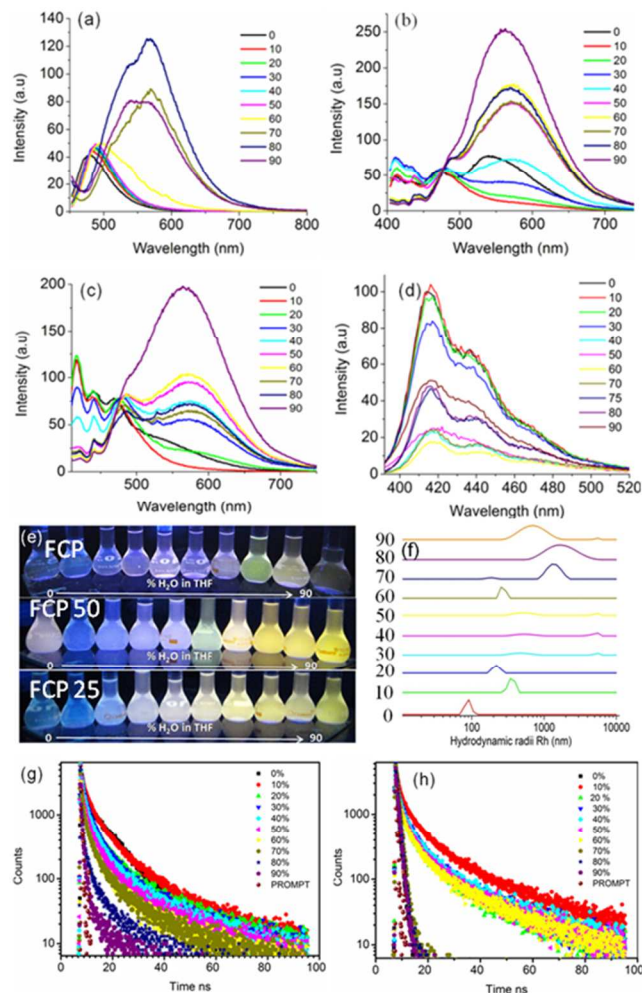

Figure 4. Photoluminescence (PL) spectra of (a) FCP monomer (excitation wavelength is = 433 nm) (b) FCP 50, (c) FCP 25, and (d) FCP 2.5 in THF and THF/Water mixtures (excitation wavelength is = 383 nm) and concentration of the solution is 4×10^{-4} g dl^{-1}; (e) photograph of FCP monomer and copolymers upon irradiation at ~360 nm in THF and THF/Water mixtures; (f) DLS traces of FCP monomer; (g) and (h) Fluorescence life time decay of FCP 50 and FCP 25.

A closer observation of Figure 4(a) showed an emission for FCP monomer in 100% THF centring at 480 nm, with low emission intensity observed. Maximum emission intensity was observed in 90% f_w in THF, centred at around 570 nm (Figure 4 (a)). The

emission of aggregates in FCP monomer revealed a bathochromic shift relative to that of respective THF solution of ~90 nm which is possibly with the J- aggregate formation and restrictions of intra molecular rotation in aggregate state.[51] From the above observation it may be concluded that FCP m

onomer possessed aggregation induced enhanced emission (AIEE) characteristics.

The DLS spectra of FCP monomer (Figure 4 (f)) indicate a higher percentage of f_w above 60% induced precipitation. The above inference is evidenced by the broadened absorption spectra and higher hydrodynamic radii for FCP monomer in water/THF mixtures with f_w >60%.

The emission spectra of FCP 50 and FCP 25 showed interesting result of AIEE phenomena with double emission. Addition of water into the THF solution resulted in emission enhancement with red shift relative to that of THF solution indicating J- aggregates formation.[52] Maximum emission intensity was observed in the case of FCP 50 and FCP 25 at 90% water in THF. The corresponding results from the DLS measurement (Figure S12 (a) and (b) †) illustrate the hydrodynamic radii varying with increase in the percentage of f_w in THF/water mixture. FCP 50 elicited the presence of two peaks appearing at 238 and 18 nm in THF solution, indicating the perturbation of π aggregates in 100% THF solution owing to increased polarity and solvation.[53] At f_w 60%, the DLS result showed a broadened peak with the hydrodynamic radius value of 1000 nm. In case of polymer dispersions in 70 and 80% water containing the emission was slightly reduced and DLS indicated one broadened peak at ~1000 nm. Nevertheless, when the water composition was increased to 90%, the emission intensity reached maximum for both FCP 50 and FCP 25 with corresponding DLS traces eliciting a broad peak at around 1000 nm. This phenomenon should be attributed to the partial restriction of intramolecular rotation (RIR) in aggregate state which enhances the radiative process and simultaneously blocks the non-radiative decay of excited states.[54] In contrast to the above observation, only a partial enhancement was observed for polymers with low composition of FCP units and same trends observed in DLS. The time dependant profile of the copolymers with aggregated state for FCP 50, and FCP 25 showed a biexponential decay features with increased life time decay channels. Such lifetimes are characteristic and originate from π-π* transitions as well as the intramolecular charge transfer (Figure 4 (g), (h)). Interestingly, low percentage composition of FCP 2.5 showed highest emission intensity at f_w 10% in water/THF mixtures (Figure (4 (d)). This maximum intensity of f_w 10% can attributed to the hydrophobic nature of 9,9-dihexylfuorene moieties. While increasing the f_w in water/THF mixtures, their emission was quenched remarkably upto with f_w 60%. Then the partial emission enhancement started at f_w 70%, it was continued upto f_w 90%. The above results are well comparable with the reported polymeric AIEE system.[64] In contrast to the white light emission from the thin film state where as the solution state showed blue emission for FC 2.5. The above emission effects can be attributed to low percentage composition of FCP monomer in FCP 2.5 copolymer. This can be due to the less emissive in a polar medium and partially enhanced emission occurred with the addition of water.[47]

Thin film morphology and supramolecular assembly

The morphology of copolymers was studied using Atomic force microscopy (AFM) and the results were correlated with the Grazing Incidence X-ray Diffraction (GIXRD) data. The copolymers were found to show variation in morphology with change in percentage composition of the FCP monomeric units in polymer backbone. It is to be noted that AFM and SEM analyses exhibited circular domains with two different size ranges that are clearly visible in thin films of all copolymers (Figure 5). It is interesting to note that FCP 50 copolymer with highest composition of FCP units in main chain exhibited very prominent large numbers of smaller spherical assemblies in AFM and SEM analyses.
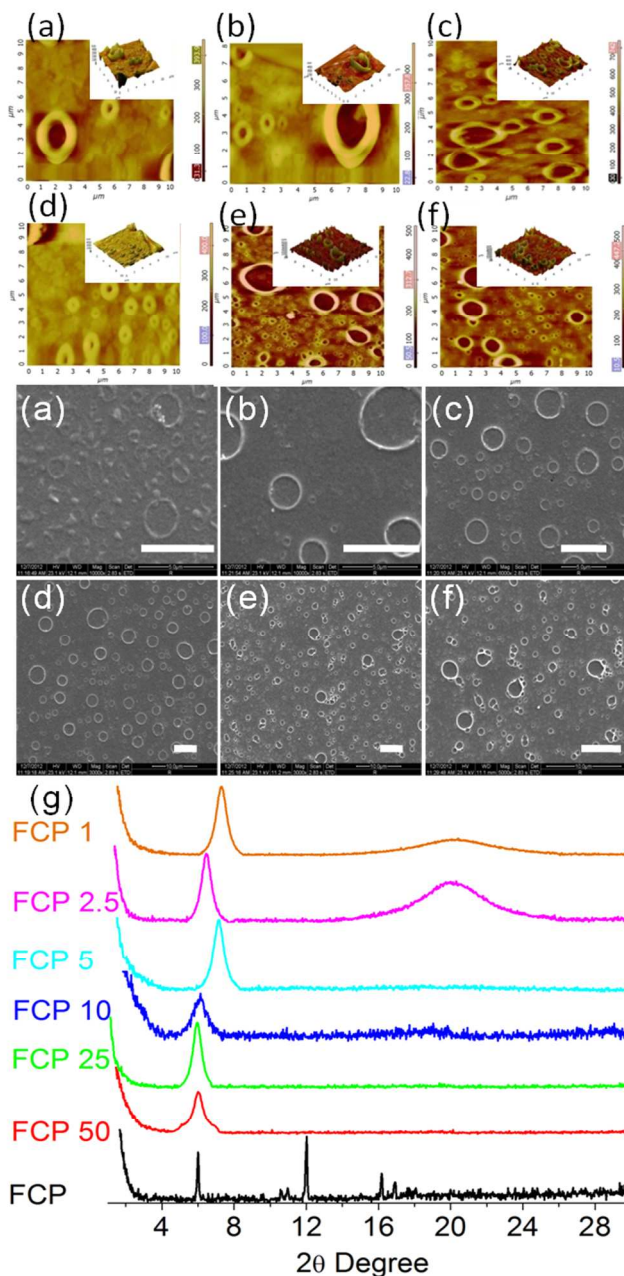

Figure 5. AFM micrograph of (a) FCP 1, (b) FCP 2.5, (c) FCP 5, (d) FCP 10, (d) FCP 25, (e) FCP 50; SEM micrograph of (a) FCP 1, (b) FCP 2.5, (c) FCP 5, (d) FCP 10, (d) FCP 25, (e) FCP 50; scale bar for all SEM images is equal to 5 μm; (g) GIXRD traces of FCP and copolymers.

It is clear from the morphological features that the composition of the FCP monomer units influenced the relative numbers of large and small spherical assemblies. FCP 50 showed large number of circular assemblies with smaller size while FCP 25 showed slight change in the morphology with relatively lesser number of small circular assemblies. In case of FCP 10, an ensemble of uniformly sized spherical assemblies was observed in spun thin films. In FCP 5 the uniformity in the size of assemblies were disturbed. In case of FCP 2.5 and FCP 1, further fewer numbers of circular assemblies with larger radii were visible signifying a marked effect of FCP content in the main chain.

The XRD traces recorded on films deposited on ITO substrates were studied to decipher more details of the intermolecular interactions (Figure 5 (g)). The monomer, FCP showed two prominent reflections at 5.97° and 12.01° corresponding to spacing of 14.8 and 7.4 Å respectively, these can be attributed to the first and second order reflections. Another less prominent reflection was observed at around 16.16° corresponding to the spacing of 5.24 Å indicating molecular level ordering.[55] The reflection observed for pure FCP monomer can be attributed to the crystallinity of film deposited. XRD traces of copolymers with higher composition of FCP units showed a very prominent reflection close to 5.90° 2θ. A similar, reflection that is broader was observed in the case of FCP 50, FCP 25 and FCP 10. However FCP 10 elicited a very weak and broad reflection peak corresponding to 19.0° and is very close to the amorphous halo observed in the case of poly 9,9-dialkylfluorene. The reflection at 5.9° vanished and a new reflection peak corresponding to 7.1° 2θ (12.44 Å) was observed in case of FCP 5 which can be attributed to the β-phase in 9, 9-dialkylfluorenes.[56] However, the characteristic amorphous halo was not observed in case of FCP 5. FCP 2.5 showed a reflection corresponding to d spacing of 12.98 Å (6.8° 2θ), which is slightly higher than the characteristic β-phase of polyfluorenes. However the amorphous halo was observed in case of FCP 2.5 copolymer. Based on the above discussions, it is clear that the composition of copolymers can be correlated with the number of observable circular assemblies in the AFM. Corresponding XRD traces showed a gradual decrease in the spacing of polymers compared to that of FCP monomer. In copolymers with lower compositions of FCP units, the molecules became closer to give an assembly similar to that in metastable β-phase. The characteristic metastable β-phase can be considered as a cause for enhanced quantum yield in thin film for all copolymers.[57]

It is probable that the composition of FCP units in the 9, 9-Dihexylfluorene backbone actuated a change in the radius of curvature of the polymer chain. It can be visualized that the alkyl chains and substituents form the core of the spherical micelles while the polyfluorene backbone form the shell.[58] It has been previously observed that rod-coil type polyfluorenes showed formation of hollow spherical micelles in THF solution.[59] An increase in the FCP units in copolymers resulted in decrease in the radius of curvature by reduced dihedral angle between polyfluorene rings. A reduced composition of FCP units resulted in increased dihedral angle between polyfluorene rings that lead to higher radius of curvature of polymer chains and hence possibly larger spherical micelles. The red shifts appeared in the aggregated state and solid films may cause by the strong inter-

molecular and/or intra-molecular interactions, e.g. strong dipole-dipole interactions, between the pendants.

Electroluminescence characteristics and decreased charge trapping

LEDs were fabricated from monomer and copolymers with device configuration ITO/PEDOT-PSS/EML/Al by solution processing technique. The LED device characteristics were studied under different conditions interestingly monomer and the copolymers were exhibited bright electroluminescence and low turn on voltage (Figure 6 (d) and (e), (Table S3 †)). The FCP monomer exhibited a bright yellow emission with CIE coordinates of (0.44, 0.49) with turn on voltage of 4.3 V. The maximum brightness of LED with FCP monomer as emissive layer was observed to be 18746 cd m^{-2} at 13.5 V. Maximum current efficiency (η^C_{max}) and power efficiency (η^P_{max}) were found to be 11.91 cd A^{-1} and 5.77 lm W^{-1} respectively. The ambipolar charge carrier mobility of FCP monomer obtained by space charge limited current (SCLC) method was found to be 2.11 x 10^{-6} S cm^{-2}.[60]

The FCP monomer with bright yellow electroluminescence was copolymerized with 9, 9-dihexylfluorene to get white light emission of varying purity as shown in (Figure 6 (a), (b)).The OLEDs fabricated from the copolymers of FCP and 9,9-dihexylfluorene elicited a broad emission due to Fluorescence Resonance Energy Transfer (FRET).[61] The copolymers, FCP 50, FCP 25 and FCP 10 exhibited a yellow emission in EL, with CIE coordinates of (0.38, 0.44), (0.36, 0.41), and (0.43, 0.42) respectively in (Figure 6 (b) and S3†)). Interestingly the PL, CIE coordinates of copolymers FCP 50, FCP 25 and FCP 10 were found to be (0.37, 0.44), (0.37, 0.43), and (0.41, 0.38) respectively. Thus the CIE coordinates in EL and PL matched very closely for copolymers FCP 50, FCP 25, FCP 10 and FCP 5 that had relatively higher composition of FCP units in backbone. The current efficiency for FCP 50, FCP 25, FCP 10 and FCP 5 were found to be 6.12, 4.79, 4.38 and 3.12 cd A^{-1} respectively. OLEDs with FCP 50, FCP 25, FCP 10 and FCP 5 as an emissive layer elicited a power efficiency of 4.83, 4.67, 3.98 and 5.93 lmW^{-1} respectively (Table S3†). Notably the copolymers, FCP 5, and FCP 1 exhibited an EL CIE coordinates of (0.30, 0.38), and (0.30, 0.31), respectively. White EL with a better purity was observed for the OLED with FCP 2.5 exhibiting a CIE coordinates of (0.33, 0.34) with obtained current efficiency and power efficiency values of 6.34 cd A^{-1} and 4.83 lm W^{-1} respectively. The maximum brightness of white LED was found to be 9332 cd m^{-2} at 12 V. The good performance of OLEDs with FCP 2.5 as emissive layer can be attributed to the energy transfer to FCP moieties in main chain. The FCP units in the copolymers being AIE active, resulted in efficient emission properties by dampening the aggregation caused quenching process in polyfluorene chain. A deconvolution of the EL spectrum of FCP 2.5 is presented in (Figure 7). It is clear that the emission can be deconvoluted into three components with blue, green and red leading to pure white light emission.

Higher current and luminous efficiency values of the OLEDs can be explained by the possible balanced charge carrier injection in copolymers as evident from the energy band diagram in (Figure 6 (c)). In contrast, the best efficiency of WOLED reported till date based on polyfluorene with napthalimide and benzothiadiazole
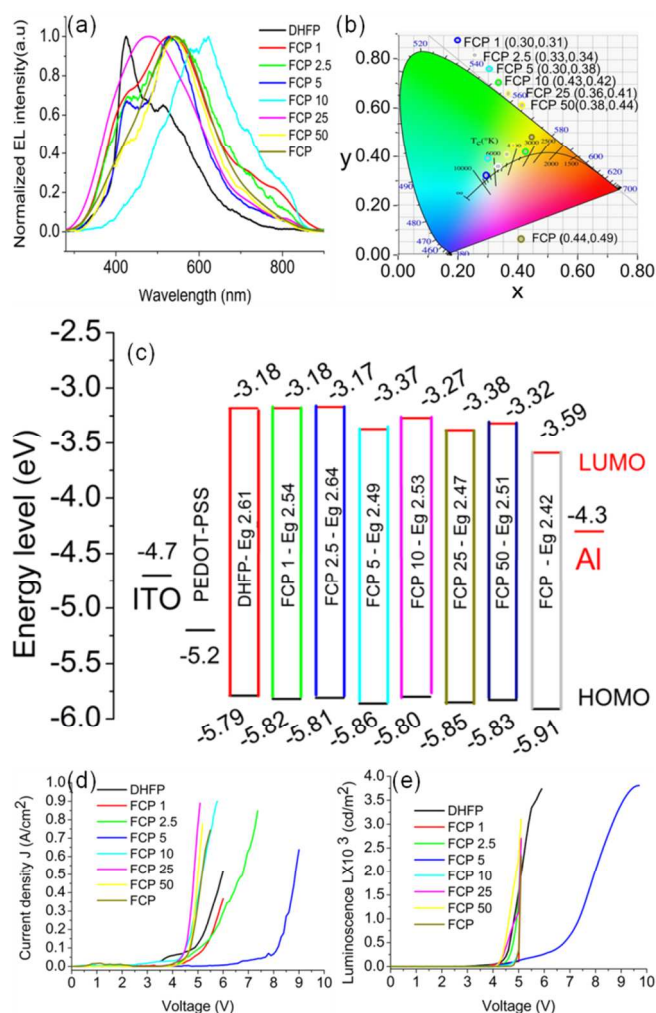
Figure 6. (a) EL spectra of FCP monomer and copolymers (b) CIE coordinates of FCP and copolymers; (c) Energy level diagram of FCP and copolymers; (d) and (e) Current density voltage (J-V) and Luminescence - voltage (L-V) plots of OLEDs for FCP and copolymers.

side chain based polymers showed an imbalance in carrier injection.[62]

Owing to the above imbalance in carrier injection, the above WOLED was reported to show predominant long wavelength emission in EL as compared to its PL spectra. The difference between PL and EL spectra of these polymers is due to charge trapping where the electronic levels of the covalent dopants are located within the band gap of host (polyfluorene) polymer system. Such observations of charge trapping was observed for white light emitting single polymers with covalent dopants in main and side chains as well.[63] In the present case, it is clear from the band diagram (Figure 6 (c)) that the energy levels of FCP units are offset from that of poly(9,9-dihexylfluorene-2,7-diyl) and hence reduced charge trapping.

Theoretical studies on monomer and copolymer

To gain insights into the structural and electronic basis for the experimental findings, geometry and electronic structure of the model systems were calculated by using the Density Functional Theory calculations. Further, excited-state vertical transitions of the model compounds were also predicted by using Time

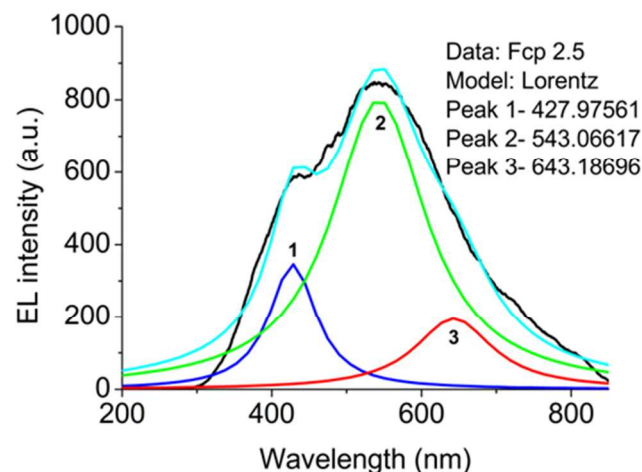Dependent Density Functional Theory (TDDFT) approach.

Figure 7. Deconvoluted EL spectrum of FCP 2.5 by Lorentz fit

Calculated structures and properties of organic electronic materials in the ground and excited states with Lee–Yang–Parr functional (B3LYP) functional often provide good agreement with experiment compared to other functional.[65-68] Hence, all the calculation were performed by B3LYP functionals.The computational details are given in supporting information. It can be seen from (Figure S14†)) that the optimized geometry of FCP containing model copolymer, (2) has twisted peripheral units with reference to the central fluorene unit. The calculated electron density distributions of frontier molecular orbitals (FMO) are depicted in (Figure 8). It is evident from (Figure 8) that, in FCP unit (1), both HOMO and LUMO are localized on the 2-Cyano-3-(4-dimethylaminophenyl) acrylic acid moiety. Close analysis of these orbitals reveals that the HOMO is predominantly localized on the electron donating amine nitrogen unit and the LUMO is mostly concentrated on the cyanoacrylic acid. As a result, there is a possibility for the intermolecular charge transfer transition between the dimethylamine to cyano acrylic acid unit. In the case of model system **(2)**, the HOMO is delocalized on the fluorene units.
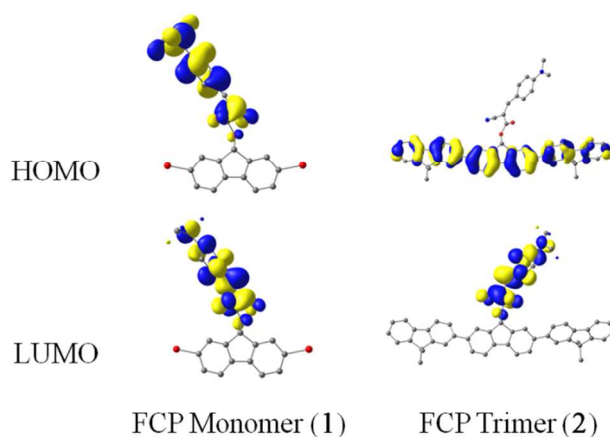

Figure 8. Topologies of frontier molecular orbitals (isosurface value=0.025 au) of FCP Monomer (1) and FCP trimer (2) calculated at the B3LYP/6-31G* level. The hydrogen atoms are omitted here for clarity.

Table 3. Summary of the excited state electronic transitions obtained from the TD-DFT calculations at B3LYP/6-31G* level.

Model systems	States	Absorption (nm)	Energy (eV)	Oscillator strength (f)	Dominant contribution (%)[a]	Exp (nm)
FCP Monomer (**1**)	S_1	391	3.17	1.1047	H→L (99%)	373
	S_4	298	4.16	0.2595	H-1→L+1 (59%), H→L+2 (26%)	
	S_7	285	4.35	0.3186	H-1→L+2 (68%), H-1→L+1 (16%)	
FCP Trimer (**2**)	S_1	435	2.85	0.0044	H→L (99%)	431
	S_2	390	3.18	0.9610	H-1→L (99%)	
	S_4	371	3.34	2.2577	H→L+1 (97%)	383

[a] H denotes HOMO and L denotes LUMO.

It is also interesting to note the presence of anti-bonding interaction between two fluorene units. The LUMO of (2) is concentrated on the 2-Cyano-3-(4-dimethylaminophenyl) acrylic acid moiety. The electron density distributions of FMO on the different subunits signify that there is an intramolecular charge transfer between fluorene to 2-Cyano-3-(4-dimethylaminophenyl) acrylic acid units in contrast to (1). The origin of the HOMO-LUMO charge density separation is clearly evident from the presence of a node on the C9 carbon of the central fluorene unit which prevents the delocalization of HOMO on the 2-Cyano-3-(4-dimethylaminophenyl)acrylic acid unit. Hence, localization of HOMO and LUMO is on the fluorene and cyanoacrylic acid units respectively. The calculated vertical excitation energies for monomer and oligomer using TDDFT approach are listed in (Table 3). Examination of the calculated values shows that the calculated spectral properties of the both monomer and oligomer are in close agreement with experimental values. For the model (1), the maximum absorption peak is predicted to be at 391 nm (f=1.1047) which arises from HOMO to LUMO transition. In (2), the maximum absorption peak is found to be at 371 nm (f=2.2577) (Figure S15†)). For the same system, the intramolecular charge transfer peak that can be seen at 431 nm (f=0.0044). This transition arises from the H→L+1 and H→L respectively. To shed more light on the transitions, the orbitals involved in the dominant excited state electronic transitions were derived from the TD-DFT calculations. The calculated values are presented in (Table 3). It can be noticed (Table 3) that for both model systems, the low energy transition arises from HOMO→LUMO (99%). Emission spectra of the model compounds (1) and (2) were calculated from the optimized excited state geometries. The calculated values are depicted in (Figure S16†)). For model system (1), LUMO→HOMO transition mainly contributes to emission at the 426 nm (f=1.0642) which is in close agreement with the experimental value of 416 nm. Similarly for model compound (2), the emission peak is observed at 420 nm (f= 0.6655) which is in very good corroboration with the experimental value of 413 nm.

Conclusion

In this work, we have proposed a new design for a fluorene-derived polymerizable AIEE luminogen, (E)-2,7-dibromo-9H-fluoren-9-yl-2-cyano-3-(dimethylamino)phenyl)acrylate (FCP) monomer. The molecule elicited a very low PL quantum yield (0.01%) in solution state that increased to 73.4% upon aggregation in solid state. A series of solution processable copolymers of FCP with 9 9'-dihexylfluorene were synthesized and their photo physical properties were investigated. The incorporation of FCP monomer in polymer backbone resulted in white light emission and enhanced quantum yield in solid films. The AIEE property in copolymers was observed for FCP 50 and FCP 25 and also the partial enhancement was happened when the FCP composition was at a minimum of 10% to 2.5%, which is comparable with previous report based on tetraphenylethylene-fluorene copolymers. A pure white light emission was observed in single copolymer, FCP 2.5. The LEDs fabricated with a device configuration of ITO/PEDOT:PSS/EML/Al with FCP 2.5 as emissive layer displayed an EL with CIE coordinates of (0.33, 0.34) that was much close to standard white light emission. The maximum brightness of 9332 cd m^{-2}, maximum power efficiency of 4.83 lm W^{-1} and maximum current efficiency of 6.34 cd A^{-1} was observed for FCP 2.5. The enhanced emission in thin film state of copolymers attributed to the supramolecular self-assembly of molecules due to FCP AIE units. Moreover the EL spectra of FCP 2.5 showed only a slight variation from PL, indicating energy transfer is the dominant process in white EL in contrast with previous reports on single layer copolymers even with an additional electron injection layer.

Experimental Section

Material and Characterization:

Tetrahydrofuran (THF), Dichloromethane (DCM), were distilled under normal pressure and then purged with nitrogen overnight before use. 2,7-dibromofluorenone, sodiumborohydride, dimethyl amino pyridine, N,N-dimethylamino-4-benzaldehyde, pyridine, 9,9-dihexylfluorene, tetrakistriphenylphosphine palladium(0) were purchased from Sigma Aldrich company and used as received for synthesis of monomer and copolymers.

1H, 13C NMR spectroscopic studies were measured on a JEOL ECA 500 MHz and Bruker NMR spectrometer using CDCl3 as a solvent and tetramethylsilane (TMS, δ = 0) as internal standard. Matrix–assisted laser desorption and Ionization (MALDI) mass spectra were recorded on Bruker ultraflexreme MALDI–mass spectrometer by using 4-HCCA (α-hydroxycinnamic acid) matrix. Elemental analyses were carried out using Euro Vector S.P.A, Euro EA 3000 CHNS elemental analyzer.

UV-Visible absorption spectra were recorded on Varian Carey 50 Bio UV-Visible spectrophotometer and photoluminescence spectra were recorded on Varian Carey eclipse fluorescence spectrophotometer using solutions for absorption and photoluminescence with concentration of 2.02×10^{-4} g dl^{-1} (monomer and copolymers). Spectral properties of thin film were studied using spin coated thin films on optically clean quartz substrates with ~1mm thickness prepared from solutions with concentration of 2 mg ml^{-1}. Cyclic voltammeter (CV) experiments were done using CH instruments, CHI 600D electrochemical work station. The conventional three electrode configuration consists of platinum disc electrode as the working electrode, Ag/AgCl electrode as reference electrode, platinum wire as counter electrode. Tetrabutylammonium hexafluorophosphate (0.1M TBAPF6) was used supporting electrolyte.

Dynamic light scattering (DLS) experiments were carried out on DLS instrument from Malvern instruments. Fluorescence life time experiments were done on IBH fluorescence life time system with pico second resolution and data analyses were done using HORIBA JOBIN YVON, decay analysis software program. Atomic force micrographs (AFM) were obtained on NOVA 1.0.26 RCI atomic force microscope with NT-MDT solver software for analysis, silicon cantilever (SII) with average frequency of 260 to 630 KHz with force constant of 28-91Nm^{-1} were used in semi contact mode. Scanning electron microscope (SEM) images were performed by FEI Quanta 200. Samples for AFM and SEM were prepared by spin coating the chloroform solution (2mg ml^{-1}). 300 micro litre of the solution was coated over the surface area of 1.7 cm^2 of ITO coated glass substrate to simulate the end use device condition. Absolute Quantum yield of electroluminescence for polymer was collected by measuring the total light output in all directions in an integrating sphere using FLUOROLOG3 (model FL3-II) fluorescence spectrophotometer from JOBIN YVON-SPEX instruments USA. GIXRD studies were performed on films of the polymers coated on ITO substrates using Bruker AX D8 advance X- ray diffractometer with Cu Kα wave length.

OLEDs of polymers for all devices were fabricated on glass substrates precoated with indium tin oxide (ITO) with a sheet resistance 10Ω/square. The substrates were cleaned with ultra purified water and were cleaned in an ultrasonic solvent bath and then baked in a heating chamber at 120 °C and treated with oxygen plasma for 25 min before use. The PEDOT-PSS (10-30 nm) solution was spin coated on cleaned ITO substrates and baked in a heating chamber at 200 °C for one hour. After the above process 300 μl of polymer solutions with 1mg/1ml concentration in CHCl$_3$ were spin coated at 2000 rpm for 60 seconds to get uniform films of polymers (with thickness 100-150 nm) and Aluminium was coated at 10^{-5} torr. Current – Voltage (I-V) characteristic were studied on Keithly 2400 source meter. Luminescence – Voltage (L-V) characteristic of OLEDs were studied using NUCLEONIX type 168 PMT housing with drawer assembly. Electroluminescence spectra of OLEDs were further measured using Carey Eclipse fluorescence spectrophotometer. Commission internationale de l' eclairage (CIE) color coordinates values of the thin films of the LEDs were standardized using Konica Minolta CS-100 Chromameter in automated mode.

Notes and references

ᵃ Council of Scientific and Industrial Research (CSIR)-CLRI, Adyar, Chennai, 600 020, India.
E-mail: nsomanathan@rediffmail.com; Fax: +91-44-24911589; Tel: +91-44-24437189.
ᵇ CSIR-Network of Institutes for Solar Energy, India.
ᶜ Academy of Scientific and Innovative Research (AcSIR), Anusandhan Bahavan, 2 Rafi Marg, New Delhi 110001, India.

† Electronic supplementary information (ESI) available: Detailed synthetic strategy and procedure for the synthesis of monomer and copolymers. ^{1}H, ^{13}C, IR and MALDI mass spectrum of Monomer and ^{1}H NMR spectrum of Copolymers, Computational details with other results of spectral and device properties are present in ESI. DOI: 10.1039/b000000x/.

1 (a) K. T. Kamtekar, A. P. Monkman and M. R. Bryce, *Adv. Mater*, 2010, **22**, 572; (b) G. M. Farinola and R. Ragni, *Chem. Soc. Rev,* 2011, **40**, 3467.

2 C. W. Tang and S. A. Vanslyke, *Appl. Phys. Lett,* 1987, **51**, 93.

3 (a) Y. G. Ma, H. Zhang, J. C. Shen and C. Che, *Synth. Met*, 1998, **94**, 245; (b) C. Adachi, M. A. Baldo, S. R. Forrest and M. E. Thompson, *J. Appl. Phys*, 1999, **11**, 285.

4 (a) Y. Cao, I. D. Parker, G. Yu, C. Zhang and A. J. Heeger, *Nature*, 1998, **397**, 414; (b) M. Wohlgenannt, K. Tandon, S. Mazumdar, S. Ramasesha and Z. V. Vardeny, *Nature*, 2001, **25**, 494; (c) Z. Shuai, D. Beljonne, R. J. Silbey and J. L. Bredas, *Phys. Rev. Lett,* 2000, **84**, 131.

5 (a) S. J. Su, E. Gonmori, H. Sarabe and J. Kido, *Adv. Mater,* 2008, **6**, 4189; (b) F. M. Hsu, C. H. Chien, C. F. Shu, C. H. Lai, C. C. Hsieh, K. W. Wang and P. T. Chou, *Adv. Funct. Mater,* 2009, **19**, 2834; (c) Y. Tao, Q. Wang, C. L. Yang, C. Zhong, K. Zhang, J. G. Qin and D. G. Ma, *Adv. Funct. Mater,* 2010, **20**, 304; (d) Y. C. Luo, H. Aziz, *Adv. Funct. Mater,* 2010, **20**, 1285; (e) S. O. Jeon, S. E. Jang, H. S. Son and J. Y. Lee, *Adv. Mater,* 2011, **23**, 1436.

6 (a) K. Goushi, K. Yoshida, K. Sato and C. Adachi, *Nat. Photonics*, 2012, **6**, 253; (b) A. Endo, K. Sato, K. Yoshimura, T. Kai, A. Kawada, H. Miyazaki and C. Adachi, *Appl. Phys. Lett,* 2011, **98**, 083302; (c) H. Uoyama, K. Goushi, K. Shizu, H. Nomura and C. Adachi, *Nature*, 2012, **492**, 234.

7 (a) S. Reineke and M. A. Baldo, *Phys. Status. Solidi A*, 2012, **12**, 2341; (b) A. P. Monkman, *ISRN Materials Science*, 2013, DOI: 10.1155/2013/670130.

8 (a) S. Reineke, F. Lindner, G. Schwartz, N. Seidler, K. Walzer, B. Lüssem and K. Leo *Nature*, 2009, **459**, 234; (b) J. Kido, M. Kimra and K. Nagai, *Science*, 1995, **267**, 1332; (c) W. Y. Wong and C. L. Ho, *J. Mater. Chem*, 2009, **19**, 4457.

9 (a) Y. Xu, J. Peng, Y. Mo, Q. Hou and Y. Cao, *Appl. Phys. Lett*, 2005, **86**, 163502; (b) Y. Zhou, Q. Sun, Z. Tan, H. Zhong, C. Yang and Y. Li, *J. Phys. Chem. C*. 2007, **111**, 6862; (c) S. Liu, F. Li, Q. Diao, Y. Ma, *Org. Electron,* 2010, **11**, 613.

10 (a) X. Gong, S. Wang, D. Moses, G. C. Bazan and A. J. Heeger, *Adv. Mater*, 2005, **17**, 2053; (b) S. Tokito, T. Iijima, T. Tsuzuki, F. Sato,

App. Phys. Let, 2003, **83**, 2459; (c) E. L. Williams, K. Haavisto, J. Li, G. E. Jabbour, *Adv. Mater,* 2007, **19**, 197.

11 (a) T. H. Kim, H. K. Lee, O. O. Park, B. D. Chin, S. H. Lee and J. K. Kim, *Adv. Funct. Mater,* 2006, **16**, 611; (b) P. I. Shih, Y. H. Tseng, F. I. Wu, A. K. Dixit and C. F. Shu, *Adv. Funct. Mater,* 2006, **16**, 1582.

12 (a) X. Gong, W. Ma, J. C. Ostrowski, G. C. Bazan, D. Moses and A. J. Heeger, *Adv. Mater,* 2004, **16**, 615; (b) M. Granstrom and O. Inganas, *Appl. Phys. Lett,* 1996, **68**, 147; (c) B. Zhang, C. Qin, J. Ding, L. Chen, Z. Xie, Y. Cheng and L. Wang, *Adv. Funct. Mater,* 2010, **20**, 2951.

13 (a) J. Huang, W. Hou, J. Li and G. Li, Y. Yang, *Appl. Phys. Lett,* 2006, **89**, 133509; (b) H. Wu, G. Zhou, J. Zou, C. Ho, W. Y. Wong, W. Yang, J. Peng and Y. Cao, *Adv. Mater,* 2008, **20**, 696; (c) F. Huang, P. Shih, C. Shu, Y. Chi and A. K. Y. Jen, *Adv. Mater,* 2009, **21**, 361.

14 (a) J-Y Lin, J. Wong, L-H. Xie, X-C Dong, and H. Y. Yang, *Macromol. Rapid Commun.* 2014, **35**, 895; (b) R. Abbel, C. Grenier, M. J. Pouderoijen, J. W. Stouwdam, P. E. L. G. Leclére, R. P. Sijbesma, E.W. Meijer and A. P. H. J. Schenning, *J. Am. Chem. Soc,* 2009, **131**, 833.

15 (a) K. I. Sakai, T. Ishikawaa and T. Akutagawa, *J. Mater. Chem. C,* 2013, **1**, 7866; (b) S. Park, J. E. Kwon, S. H. Kim, J. Seo, K. Chung, S. Y. Park, D. J. Jang, B. M. Medina, J. Gierschner and S. Y. Park, *J. Am. Chem. Soc,* 2009, **131**, 14043.

16 (a) A. Garcia, R. Yang, Y. Jin, B. Walker and T. Q. Nguyen, *Appl. Phys. Lett,* 2007, **91**, 153502; (b) B. W. D'Andrade and S. R. Forrest, *Adv. Mater,* 2004, **16**, 1585; (c) S. Chen, Q. Wu, M. Kong, X. Zhao, Z. Yu, P. Jiaa and W. Huang, *J. Mater. Chem. C,* 2013, **1**, 3508.

17 (a) S. A. Chen, K. R. Chuang, C. I. Chao, H. T. Lee, *Synth. Met,* 1996, **82**, 207; (b) C. I. Chao, S. A. Chen, *Appl. Phys. Lett,* 1998, **73**, 426; c) K. L. Paik, N. S. Baek, H. K. Kim, J-H. Lee and H. Lee, *Macromolecules,* 2002, **35**, 6782.

18 (a) M. L. Tsai, C. Y. Liu, M. A. Hsu and T. J. Chow, *Appl. Phys. Lett,* 2003, **82**, 550; (b) Y. Z. Lee, X. W. Chen, M. C. Chen, S. A. Chen, J. H. Hsu and W. S. Fann, *Appl. Phys. Lett,* 2001, **79**, 308; (c) P. T. Furuta, L. Deng, S. Garon, M. E. Thompson and J. M. Fréchet, *J. Am. Chem. Soc,* 2004, **126**, 15388.

19 V. Lukeš, R. Šolc, H. Lischka and H. F. Kauffmann, *J. Phys. Chem. A,* 2009, **113**, 14141.

22 (a) W. C. Wu, W. Y. Lee and W. C. Chen, *Macromol. Chem. Phys,* 2006, **207**, 1131; (b) L. Zhang, S. Hu, J. Chen, Z. Chen, H. Wu, J. Peng and Y. Cao, *Adv. Funct. Mater,* 2011, **21**, 3760.

23 J. Liu, Q. Zhou, Y. Cheng, Y. Geng, L. Wang, D. Ma, X. Jing and F. Wang, *Adv. Mater,* 2005, **17**, 2974.

24 (a) C. H. Chien, S. F. Liao, C. H. Wu, C. F. Shu, S. Y. Chang, Y. Chi, P. T. Chou and C. H. Lai, *Adv. Funct. Mater,* 2008, **18**, 1430; (b) J. Jiang, Y. Xu, W. Yang, R. Guan, Z. Liu, H. Zhen and Y. Cao, *Adv. Mater,* 2006, **18**, 1769.

25 X. Yang, G. Zhou and W. Y. Wong, *J. Mater. Chem.C.* 2014, **2**, 1760.

26 C. Y. Chuang, P. I. Shih, C. H. Chien, F. I. Wu and C. F. Shu, *Macromolecules,* 2007, **40**, 247.

27 J. Luo, Z. Xie, J. W. Y. Lam, L. Cheng, H. Chen, C. Qiu, H. S. Kwok, X. Zhan, Y. Liu, D. Zhu and B. Z. Tang, *Chem. Commun,* 2001, 1740.

28 S. W. Thomas, G. D. Joly and T. M. Swager, *Chem. Rev,* 2007, **107**, 1339.

29 (a) B. K. An, S. K. Kwon, S. D. Jung and S. Y. Park, *J. Am. Chem. Soc,* 2002, **124**, 14410; (b) S. Mizukami, H. Houjou, K. Sugaya, E. Koyama, H. Tokuhisa, T. Sasaki and M.Kanesato, *Chem. Mater,* 2005, **17**, 50; (c) Y. Liu, X. T. Tao, F. Z. Wang, J. H. Shi, J. L. Sun, W. T. Yu, Y. Ren, D. C. Zou and M. H. Jiang, *J. Phys. Chem. C,* 2007, **111**, 6544.

30 (a) G. Yu, S. W. Yin, Y. Q. Liu, Z. G. Shuai and D. B. Zhu, *J. Am. Chem. Soc,* 2003, **125**, 14816; (b) Z. J. Ning, Z. Chen, Q. Zhang, Y. L. Yan, S. X. Qian, Y. Cao and H. Tian, *Adv. Funct. Mater,* 2007, **17**, 3799; (c) M. Chen, L. Li, H. Nie, J. Tong, L. Yan, B. Xu, J. Z. Sun, W. Tian, Z.. Zhao, A. Qin and B. Z. Tang, *Chem. Sci,* 2015, **6**, 1932.

31 (a) R. Hu, N. L. C. Leungb and B. Z. Tang, *Chem. Soc. Rev,* 2014, **43**, 4494; (b) Y. Bao, T. Wang, Q. Li, F. Du, R. Bai, M. Smet and W. Dehaen, *Polym. Chem,* 2014, **5**, 792; (c) H. J. Yen, C. J. Chen and G. S. Liou, *Chem. Commun,* 2013, **49**, 630.

32 (a) W. Qin, K. Li, G. Feng, M. Li, Z. Yang, B. Liu, B. Z. Tang, *Adv. Funct. Mater,* 2014, **24**, 635; (b) M. Wang, D. Q. Zhang, G. X. Zhang and D. B. Zhu, *Chem. Commun,* 2008, **37**, 4469.

33 (a) C. Li, T. Wu, C. Hong, G. Zhang and S. Liu, *Angew. Chem. Int. Ed,* 2012, **51**, 455; (b) J. Wang, J. Mei, W. Yuan, P. Lu, A. Qin, J. Sun, Y. Mac and B. Z. Tang, *J. Mater. Chem,* 2011, **21**, 4056; (c) Z. Liu, W. Xue, Z. Cai, G. Zhang and D. Zhang, *J. Mater. Che,.* 2011, **21**, 14487; (d) Y. W. Lai, S. W. Kuo and J. L. Hong, *RSC Adv,* 2012, **2**, 8194; (e) X. Zhang, X. Zhang, B. Yang, J. Hui, M. Liu, Z. Chi, S. Liu, J. Xuc and Y. Wei, *J. Mater. Chem,* 2014, **2**, 816.

34 (a) W. Jia, P. Yang, J. Li, Z. Yin, L. Kong, H. Lu, Z. Ge, Y. Wu, X. Hao and J. Yang, *Polym. Chem,* 2014, **5**, 2282; (b) W. Wu, S. Ye, L. Huang, L. Xiao, Y. Fu, Q. Huang, G. Yu, Y. Liu, J. Qin, Q. Lia and Z. Li, *J. Mater. Chem,* 2012, **22**, 6374.

35 S. K. Samantha and S, Bhattacharya, *J. Mater. Chem,* 2012, **22**, 25277.

36 (a) X. Liu, J. Jiao, X. Jiang, J. Li, Y. Cheng and C. Zhu, *J. Mater. Chem. C,* 2013, **1**, 4713; (b) Y. W. Lai, S. W. Kuo and J. L. Hong, *RSC Adv,* 2012, **2**, 8194; (c) J. Chen, H. S. Kwok and B. Z. Tang, *J. Polym. Sci. Part A. Polymer Chem,* 2006, **44**, 2487; (d) C. T. Lai and J. L. Hong, *J. Mater. Chem,* 2012, **22**, 9546.

37 Y. Hong, Jacky W. Y. Lam and B. Z. Tang, *Chem. Soc. Rev,* 2011, **40**, 5361.

38 W. Z. Yuan, Y. Gong, S. Chen, X. Y. Shen, J. W. Y. Lam, P. Lu, Y. Lu, Z. Wang, R. Hu, N. Xie, H. S. Kwok, Y. Zhang, J. Z. Sun and B. Z. Tang, *Chem. Mater,* 2012, **24**, 1518.

39 (a) J. Kalinowski, M. Cocchi, D. Virgili, V. Fattori and A.G. Williams, *Adv. Mater,* 2007, **19**, 4000, (b) G. Zhou, Q. Wang, C. L. Ho, W. Y. Wong, D. Ma and L. Wang, *Chem. Commun,* 2009, 3574; (c) G. Zhou, Q. Wang, X. Wang, C.L. Ho, W.Y. Wong, D. Ma, L. Wang and Z. Lin, *J. Mater. Chem,* 2010, **20**, 7472.

40 W. Li , Y. Pan , R. Xiao , Q. Peng , S. Zhang , D. Ma , F. Li , F. Shen , Y. Wang , B. Yang and Y. Ma, *Adv. Funct. Mater,* 2014, **24**, 1609.

41 J. Shi, Y. Wu, S. Sun, B. Tong, J. Zhi and Y. Dong, *J. Polym. Sci. Part A: Polym. Chem,* 2013, **61**, 229.

42 (a) J. W. Chen, C. C. W. Law, J. W. Y. Lam, Y. P. Dong, S. M. F. Lo, I. D. Williams, D. B. Zhu and B. Z. Tang, *Chem. Mater,* 2003, **15**, 1535; (b) Y. Hong, J. W. Y. Lam and B. Z. Tang, *Chem. Commun* 2009, 4332; (c) B. Chen, H. Nie, P. Lu, J. Zhou, A. Qin, H. Qiu, Z. Zhao and B. Z. Tang. *Chem. Commun,* 2014, **50**, 4500; (d) R. Hu, N. L. C. Leung and B. Z. Tang, *Chem. Soc. Rev,* 2014, **43**, 4494.

43 Z. R. Grabowski, K. Rotkiewicz and W. Rettig, *Chem. Rev,* 2003, **103**, 3899.

44 (a) C. Y. Sun, X. L. Wang, X. Zhang, C. Qin, P. Li, Z. M. Su, D. X. Zhu, G. G. Shan, K. Z. Shao, H. Wu and J. Li, *Nat. Commun,* 2013, **4**, 271; (b) A. Shao, Z. Guo, S. Zhu, S. Zhu, P. Shi, H. Tiana and W. Zhu, *Chem. Sci,* 2014, **5**. 1383.

45 V. Petta, J. Moradian-Oldak, S. N. Yannopoulos and N. Bouropoulos, *Eur. J. Oral Sci,* 2006, **114**, 308.

46 (a) C. Suryanarayanan, E. Ravindran, S. J. Ananthakrishnan, N. Somanathan and A. B. Mandal, *J. Mater. Chem,* 2012, **22**, 18975; (b) J.M. Thomas and S. Reinhard, *J. Am. Chem. Soc,* 2011, **133**, 1066; (c) D. Chang, H. Shen, G. Li, B. Zhao, A. Yu, Q. Zhao and H.Wang, *Anal. Chem,* 2012, **84**, 8088.

47 (a) Y. Ren, J. W. Y. Lam, Y. Dong, B. Z. Tang and K. S. Wong, *J. Phys. Chem. B,* 2005, **109**, 1135; (b) S. J. Ananthakrishnan, E. Varathan, N. Somanathan, V. Subramanian and A. B. Mandal, J. D. Sudha, R. Ramakrishnan, *J. Mater. Chem. C,* 2014, **2**, 9035.

48 J. Geng, K. Li, W. Qin, L. Ma, G. G. Gurzadyan, B. Z. Tang and B. Liu, Small, 2013, **11**, 2012.

49 (a) B. K. An, S. K. Kwon, S. D. Jung and S. Y. Park, *J. Am. Chem. Soc,* 2002, **124**, 14410; (b) J. Xu, L. Wen, W. Zhou, J. Lv, Y. Guo, M. Zhu, H. Liu, Y. Li and L. Jiang, *J. Phys. Chem. C,* 2009, **113**, 5924; (c) S. Jayanty and T. P. Radhakrishnan, *Chem. Eur. J,* 2004, **10**, 791.

50 A. Qin, C. K. W. Jim, Y. Tang, J. W. Y. Lam, J. Liu, F. Mahtab, P. Gao and B. Z. Tang, *J. Phys. Chem. B,* 2008, **112**, 9281.

51 (a) X. Yao, X. Ma and H. Tian, *J. Mater. Chem. C,* 2014, **2**, 5155; (b) Y. Hong, J. W. Y. Lamab and B. Z. Tang, *Chem. Soc. Rev,* 2011, **40**, 5361; (c) L. M. Ilharco and R. Brito de Barros, *Langmuir,* 2000, **16**, 9331; (d) Z. Zhao, P. Lu, J. W. Y. Lam, Z. Wang, C. Y. K. Chan, H.

H. Y. Sung, I. D. Williams, Y. Mab and B. Z. Tang, *Chem. Sci*, 2011, **2**, 672.

52 M. P. Aldred, C . Li, G. F. Zhang, W. L. Gong, A. D. Q. Li, Y. Dai, D. Ma and M. Q. Zhu, *J. Mater. Chem,* 2012, **22**, 7515.

53 S. J. Ananthakrishnan, E. Varathan, E. Ravindran, N. Somanathan, V.Subramanian, A. B. Mandal, J. D. Sudha and R. Ramakrishnan, *Chem. Commun*, 2013, **49**, 10742.

54 (a) Y. Liu, X. Feng, Shi, J. Zhi, J. Tong, B. Dong and Y. Chin. *J. Polym. Sci*, 2012, **30**, 443; (b) J. Shi, Y. Wu, S. Sun, B. Tong, J. Zhi and Y. Dong *J. Polymer. Science. Part A: Polymer Chemistry,* 2013, **51**, 229.

55 A. K. Boal, F. Ilhan, J. E. DeRouchey, T. T. Albrecht, T. P. Russell and V. M. Rotello, *Nature*, 2000, **404**, 746.

56 (a) M. J. Winokur, J. Slinker and D. L. Huber, *Phys. Rev. B,* 2003, **67**,184106; (b) M. H. Rahman, C. Y. Chen, S. C. Liao, H. L. Chen, C. S. Tsao, J. H. Chen, J. L. Liao, V. A. Ivanov and S. A. Chen, *Macromolecules*, 2007, **40**, 6572; (c) D. W. Bright, F. B. Dias, F. Galbrecht, U. Scherf and A. P. Monkman, *Adv. Funct. Mater*, 2009, **19**, 67.

57 (a) S. Kawana, M. Durrell, J. Lu, J. E. Macdonald, M. Grell, D. D. C. Bradley, P. C. Jukes, R. A. L. Jones and S. L. Bennett, *Polymer,* 2002, **43**, 1907; (b) A. J. Cadby, P. A. Lane, H. Mellor, S. J. Martin, M. Grell, C. Giebeler and D. D. C. Bradley, *Phys Rev B,* 2000, **62,** 15604.

58 Y. Tian, C. Yi Chen, H. Lap Yip, W. Chung Wu, W. Chang Chen and A. K. Y. Jen, *Macromolecules*, 2010, **43**, 282.

59 (a) Y.C. Tung and W. C. Chen, *Reactive & Functional Polymers*, 2009**, 69**, 507; (b) J. Hu, G. Zhang, Y. Geng and S. Liu, *Macromolecules*, 2011, **44**, 8207; (c) J. J. Wang, Y. N. Zhou, P. Wanga and Z. H. Luo, *RSC Adv*, 2013, **3**, 5045.

60 (a) L. Xu, Y. Li, R. Hu, S. Li, A. Qin, B. Z. Tang and B. Su, *Analyst*, 2014, **139**, 2332; (b) G. Liu, M. Yang, L. Wang, J. Zheng, H. Zhou and J. W, Y. Tian, *J. Mater. Chem. C*, 2014, **2**, 2684; (c) M. X. Gao, C. Fang Liu, Z. Li. Wu, Q. L. Zeng, X. X. Yang, W. B. Wu, Y. F. Li and C. Z. Huang, *Chem. Commun*, 2013, **49**, 8015; c) W. Qin, D. Ding, J. Liu, W. Z. Yuan, Y. Hu, B. Liu, B. Z. Tang, *Adv. Funct. Mater*, 2012, **22**, 771.

61 C. wu, W. Y. Lee, C. L. Pai, W. C. Chen, C. S. Tuan and J. L. Lin, *J. Polym. Sci, Part B: Poly. Phys*, 2006, **45**, 67.

62 J. Liu, Q. Zhou, Y. Cheng, Y. Geng, L. Wang, D. Ma, X. Jing and F. Wang, *Adv. Funct. Mater*, 2006, **16**, 957.

63 B. Zhang, C. Qin, J. Ding, L. Chen, Z. Xie, Y. Cheng and L. Wang, *Adv. Funct. Mater*, 2010, **20**, 2951.

64 J. Shi, Y. Wu, S. Sun, B. Tong, J. Zhi and Y. Dong, *J. Polym. Sci. Part A: Polym. Chem*, 2013, **61**, 229.

65 D. Vijay, E. Varathan, V. Subramanian, *J. Mater. Chem. A*, 2013, **1**, 4358.

66 E. Varathan, D. Vijay, P. S. V. Kumar and V. Subramanian, *J. Mater.Chem. C*, 2013, **1**, 4261.

67 E. Varathan, D. Vijay, V. Subramanian, *J. Phys. Chem. C* 2014, **118**, 21741.

68 M. Malagoli and J. L. Brédas, *Chem. Phys. Lett*., 2000, **327**, 13.

White Light Emitting Single Polymer from Aggregation Enhanced Emission: A Strategy through Supra molecular Assembly